International Journal of Earth Sciences Knowledge and Applications
journal homepage: http://www.ijeska.com/index.php/ijeska

Research Article

e-ISSN: 2687-5993

The Conventional Core Analysis Study for Reservoir Quality of the Well-X, Rawat Rift Basin, Sudan

Sadam H.M.A. Eltayib[1]*

[1]*Omdurman Islamic University, Department of Geology Faculty of Science and Technology-Omdurman, Khartoum, Sudan*

INFORMATION

Article history
Received 22 October 2024
Revised 27 November 2024
Accepted 28 November 2024

Keywords
Rawat Basin
Core
Porosity
Permeability
Reservoir

Contact
*Sadam H.M.A. Eltayib
sadam_h3@yahoo.com

ABSTRACT

This paper is focused on the Rawat Basin is a late Cretaceous to early Tertiary rift basin in interior Sudan. The basin is filled with continental sediments of fluvial and lacustrine sandstones, mudstones and local tuffs. Facies distribution is influenced by fault-controlled subsidence followed by prolonged episodes of thermal subsidence. The conventional core analyses study for the selected core plug samples from the cored intervals Core #1 (1441.30-1446.43 m), Core#2 (1451.86 – 1457.64 m) and Core#2 (1478.10 – 1484.70 m). The main results of this study refer that the helium porosity value for the studied plug samples ranged between 16.91% and 38.43%. . The gas permeability value for the studied plug samples ranged between 7.09 to 1668.59 MD. The residual fluid saturation values varied from 0.43% to 60.72 % for oil and 10.75 % to 77.69% for water. The grain density values varied from 2.61 g/cc to 2.67 g/cc. This result showed a very good reservoir quality.

1. Introduction

The Rawat sub-Basin lies in the northern part of Block 25 in Sudan, around 350 km south of Khartoum City between latitudes 11.6–12.8 N and longitudes 31.6–32.9 E (Fig. 1). It is located around 400 km to the southeast of the Central African Shear Zone (CASZ) and represents the northern extension of the Rawat sub-Basin. It is up to 175km long and 50 km wide and locally contains up to 6000 m of Upper Cretaceous to Neogene Sediments (Awad, 1994).

An extensive exploration campaigns have been carried-out by the operators in the Rawat Basin in interior Sudan during the last few decades. This effort resulted in identifications, drilling and discovery of hydrocarbons in most of the sizeable structural traps (Hassan, 2016). The remaining potential hydrocarbon volumes are expected to be in small-size structural traps. Recent integrated seismic mapping, petroleum system analysis and modeling studies indicate the potential exist for discovery of sizeable hydrocarbon volumes in combination structural/stratigraphic and in unstructured/stratigraphic traps. Historically these types of traps were avoided due to their high risk of failure (Awad, 1994). The tectonic evolution of the Interior Rift Basins in Sudan can be divided into a pre-rifting phase, three rifting phases, and a sag phase (Schull, 1988). The first phase of rifting started in the Late Jurassic (?) to Early Cretaceous (130-160 Ma) and terminated near the end of the Albian. The second rifting phase took place during the Turonian to Late Senonian, accompanied by minor volcanic activity and deposition of lacustrine, floodplain claystones and siltstones. Andesitic basalt encountered within the Rawat Formation in well AY-1 dated as Campanian , may be related to this phase of rifting (Salama, 1984).

The end of this phase is marked by the deposition of an increasingly sand-rich sequence that concluded with the thick Paleocene sandstone sequence of the Yale Formation. The final rifting phase began in the Late Eocene to Oligocene. This phase is reflected in the thick sequence of lacustrine and floodplain claystones and siltstones of the Adar Formation.

Since Mid-Miocene, the area has undergone gentle subsidence with little or no faulting (Bosworth, 1992).

2. General Stratigraphy

The Rawat basin is divided into five sub-basins; each is filled with continental sediments of fluvial and lacustrine sandstones, mudstones, and local tuffs (Fig. 2). Sedimentary facies distribution is mainly controlled by subsidence along faults. The active faulting was followed by a prolonged episode of thermal subsidence. The primary hydrocarbon reservoir targets are in the Upper Cretaceous formations that comprise Galhak Sand, Galhak Oil Units and sands deposited in lacustrine fans at the base of the Galhak Shale source interval (Awad, 1994), (Fig. 2).

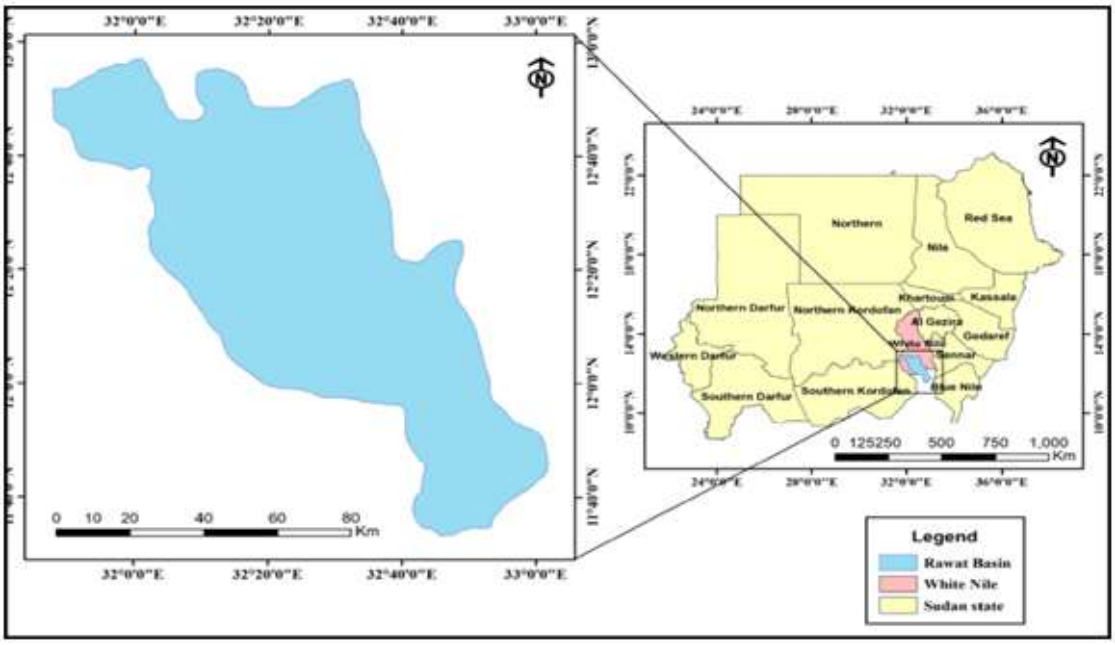

Fig. 1. Location map of study area

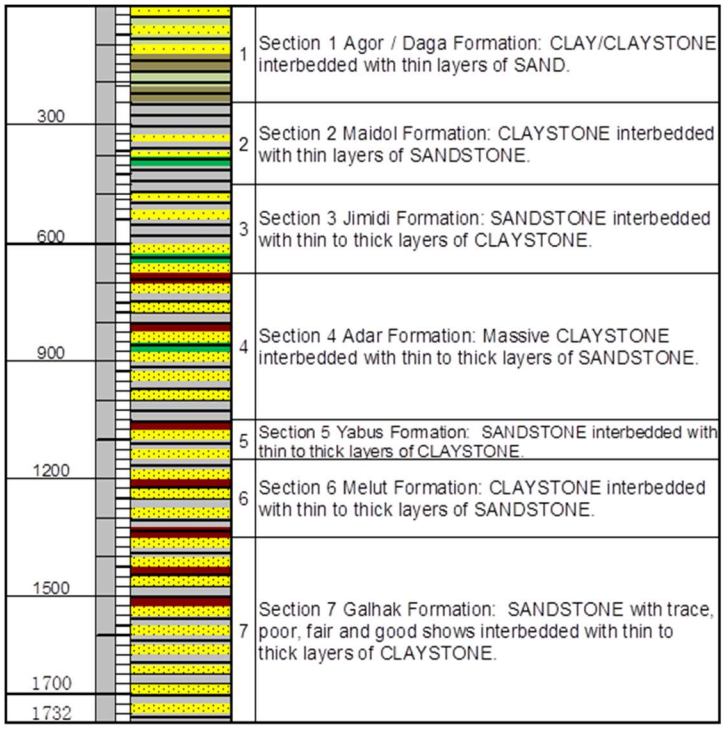

Fig. 2. Generalized stratigraphic column of study area

Tectonic subsidence played a primary controlling factor in the maturation of the hydrocarbon source sediments and the distribution of oil pools in the basin especially in the east slope of the central sub-basin. The hanging wall fault blocks

are important in the Rawat central sub-basin as proved by the presence of several hydrocarbon discoveries in such setup.

The Rawat Basin is characterized by having relatively steeper dips and high relief structural flanks. As such, it is of paramount importance to have competent top, lateral and base seals for successful hydrocarbon entrapment. To maximize our understating and reduce the geological uncertainties related to seal & hydrocarbon migration, our methodology and mitigation work were focused on identifying isolated sandstone bodies embedded within the Upper Cretaceous Galhak source rock formation.

Consequently, a Sequence Stratigraphic model was built in the study area to help predict the distribution and the quality of reservoir sands. The sequence stratigraphic model also led to better understanding of the distribution and effectiveness of the other petroleum system elements such as the source, and the seal. The integration of chronostratigraphic slicing and sequence stratigraphic work resulted in identification of potential stratigraphic traps in an area with sub lacustrine fan-like depositional feature. Eight formations have been identified for the Rawat sub-Basin and then omenclature is the same with those formations of Melut Basin. These formations; from older to younger are Gelhak, Melut, Yabus, Adar, Jimidi, Miadol, Daga and Agor (Hassan, 2016), (Fig.2).

3. Objectives of this Study

The main objectives of the core in this study are:

- Spectral Core Gamma,
- Dean and Stark fluid saturations
- Porosity, Permeability and Grain density for core plugs.

4. Material and Method

The cores were received in 1-meter lengths and (6) inches diameter fiber glass tube liners. The core was laid out on the tables to give a continuous run and were oriented by PLRS geologists. So that the maximum apparent dip of any bedding or dominant fracture trend ran from top left to bottom right of the core. The cores were then marked up with tramlines, red on the right and yellow on the left when viewing the upper surface of the orientated core from the bottom up. The following Depth intervals were recorded (Figs. 3–5):

- Core # 1 1441.30 – 1446.43 /m
- Core # 2 1451.86 – 1457.64 /m
- Core # 3 1478.10 – 1484.70 /m

5. Results and Discussion

5.1. Helium Porosity and Grain Density

The grain volumes of the horizontal plug samples were measured using a calibrated double cell Helium gas volume expansion porosimeter. Prior to each set of data (25 samples maximum) the porosimeter was checked for potential leaks, this was done by performing a 'dummy 'expansion with a steel blank in the matrix cup. The apparatus was then calibrated using seven stainless steel discs of known volumes and the relationship between pressure and volume (which is ideally linear) was calculated. The porosimeter operates using the principle of Boyle's law. The apparatus is composed of a reference cell and a sample cup, the sealed reference cell is filled with helium gas at room temperature to a pressure of approximately 9 bars. The valve between the reference cell and the sample cup will be opened to allow the gas to expand into the two cells. From Boyle's law, the grain volume of the sample can be calculated if the volume of the reference cell, the initial pressure and the final pressure are known.

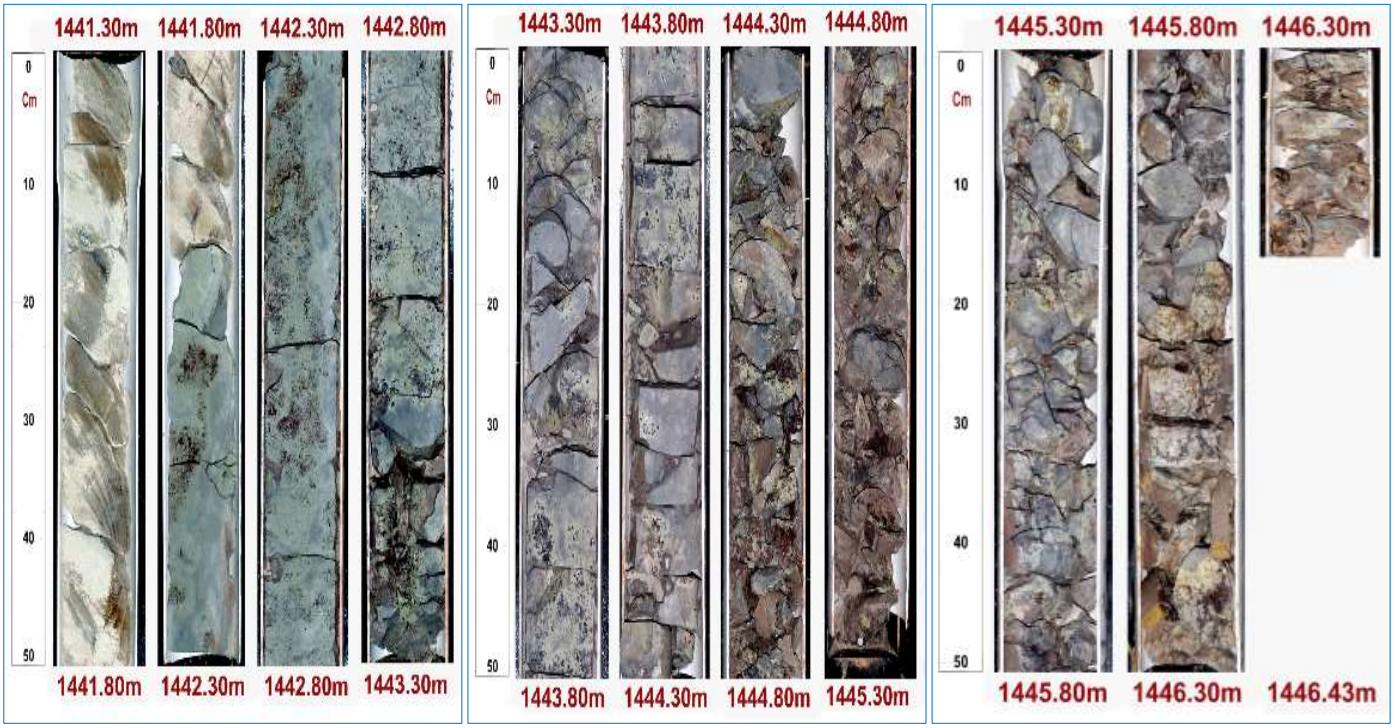

Fig. 3. Photograph showing Core # 1, interval 1441.30–1446.43 m

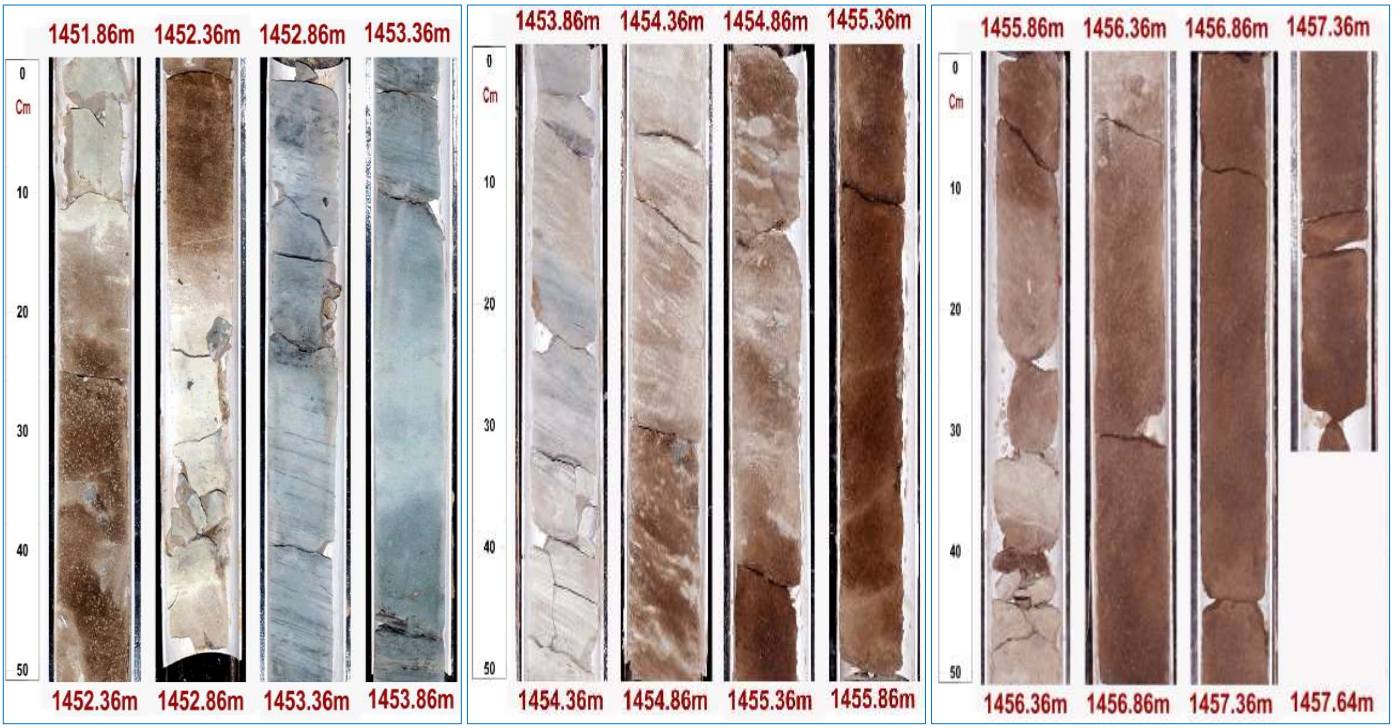

Fig. 4. Photograph showing Core # 1, interval 1451.86–1457.64 m

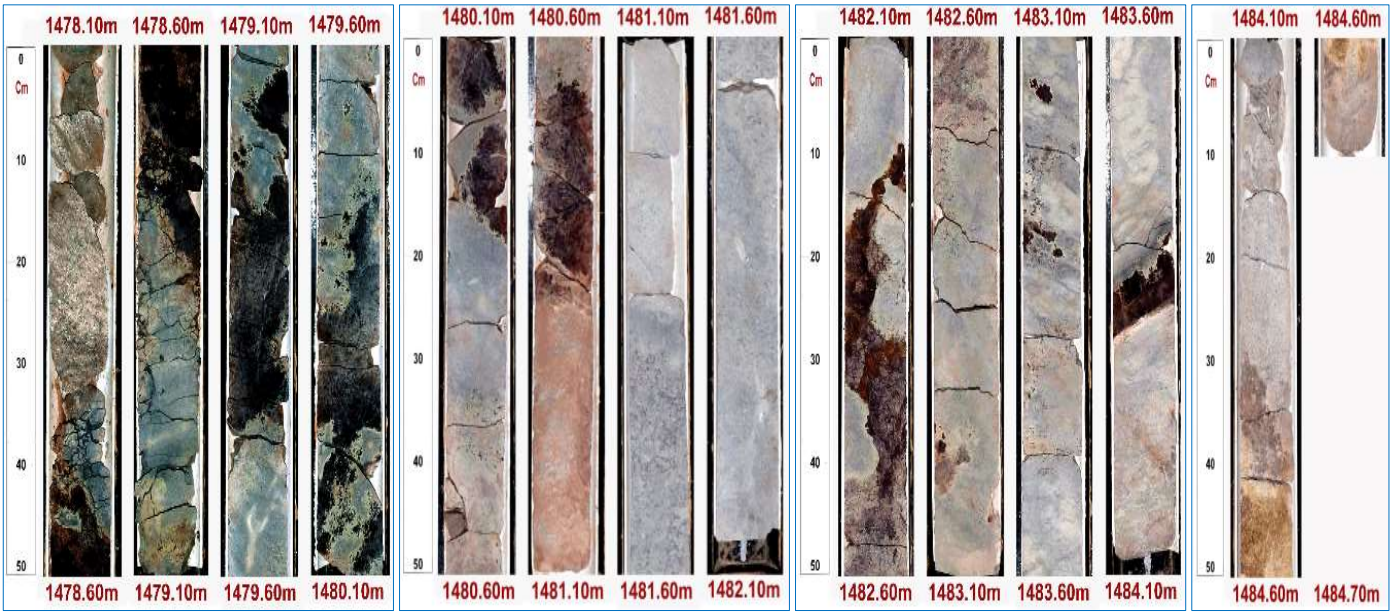

Fig. 5. Photograph showing Core # 1, interval 1478.10–1484.70 m

Subsequently the samples were loaded into the matrix cup and the procedure of helium expansion followed as described above. By using the calibration curve a grain volume is determined and recorded for each sample. The helium porosity value for the studied plug samples ranged between 16.91% and 38.43%. The grain density values varied from 2.61 g/cc to 2.67 g/cc (Figs. 6–8 and Table 1–2).

5.1.1. Bulk Volume Measurement of Consolidated Samples

Bulk volume was calculated by caliper method. The length and diameter of each core plug is measured at different points of the core plug and averaged values are determined. By determining the bulk volume and weight of the plug, the porosity and grain density of the sample were calculated.

As a quality check, a suite of standard samples of known porosities and grain densities were measured every 25 samples (Fig. 6 and Table 1–2).

5.1.2. Bulk Volume Measurement of mounted Samples

Bulk volumes were calculated by direct summation of grain volume and pore volume (since the samples were jacketed,

bulk volume measurement by mercury displacement was not possible). By determining the bulk volume and weight of the plug, the porosity and grain density of the sample was calculated. As a quality check, a suite of standard samples of known porosities and grain densities were measured every 25 samples. Upon completion of the analysis 10 % of the samples and any with anomalous results, were re-analyzed as a quality assurance check. Industry standard as outlined in (API RP 40) require porosity and grain density data to fall within a margin of error of ± 0.2 porosity units and ± 0.01 g/cc grain density of the reported value (Fig. 6 and Table 1).

5.2. Gas Permeability

Gas permeability was measured using Digital Gas Permeameter with nitrogen gas as the flowing medium. The sample was placed in a Hassler type core holder and the Hassler pressure used was 400 psi. The flow was allowed to stabilize before the readings were taken. To check the performance of the permeameter a full set of check plugs of known permeability (ranging from less than one millidarcy to 5 Darcy) was run prior to usage. When the analysis was completed 10 % of the samples, and any with anomalous results, were reanalyzed as a quality assurance check. Industry standard as outlined in (API RP 40) require data to fall within a margin of error ± 5% of the reported value. The gas permeability value for the studied plug samples ranged between 7.09 to 1668.59 MD (Fig. 6 and Table 1).

5.3. Klinkenberg Corrected Gas Permeability

Klinkenberg has reported variations in permeability determined using gases as the flowing fluid from that obtained when using non-reactive liquids. These variations were ascribed to slippage, a phenomenon well known with respect to gas flow in capillary tubes. The phenomenon of gas slippage occurs when the diameter of the capillary openings approaches the mean free path of the gas. The mean free path of a gas is a function of the molecular size and' the kinetic energy of the gas.

Therefore, the "Klinkenberg effect" is a function of the gas with which the permeability of the porous medium is determined. Upon plotting the gas permeability as a function of the reciprocal of the mean pressure of the test it was found that the extrapolated lines to infinite mean pressure when using different gases intercept the permeability axis at a common point. This point is designated KL or the equivalent liquid permeability (Fig. 6 and Table 1).

5.4. Calculation of Fluid Saturations

The residual fluid saturations values represent the volumes of water and oil that remain in the core itself. It does not account for any oil or water that is lost during the coring and core recovery process. The residual fluid saturation values varied from 0.43% to 60.72 % for oil and 10.75 % to 77.69% for water (Figs. 7–8 and Table 2).

Table 1. Statistical analysis result

Core Number	TOP (meter)	Bottom (meter)	Number of Samples	Horizontal Permeability, mD			Number of Samples	Porosity (%)		
				Max	Min	Geo Mean		Max	Min	Arithmetic Mean
1	1441.30	1446.43	3	42.70	11.09	18.57	3	22.56	20.49	21.68
2	1451.86	1457.64	14	1668.59	7.09	217.57	14	38.43	16.91	28.17
3	1478.10	1484.70	4	37.02	9.66	16.77	4	1983	18.03	18.78

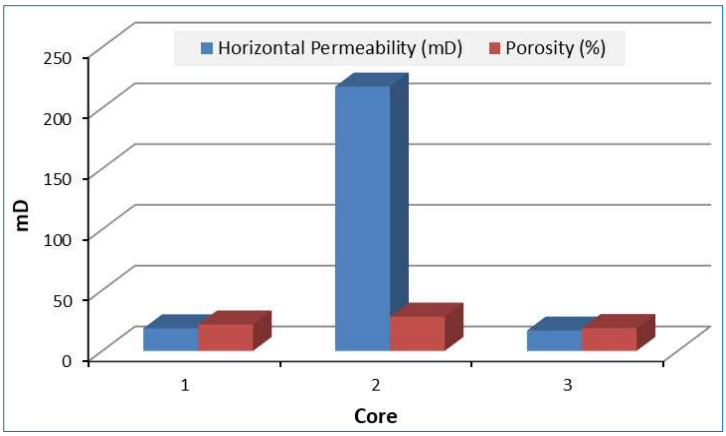

Fig. 6. Histogram showing the relation between porosity and horizontal permeability

Table 2. Statistical analysis results

Core Number	TOP (meter)	Bottom (meter)	Number of Samples	Grain Density (gm/cc)			Residual Fluid Saturations (%)					
							Oil		Water		Oil	Water
				Max	Min	Average	Max	Min	Max	Min	Average	
1	1441.30	1446.43	3	2.63	2.62	2.62	6.13	0.43	71.50	61.81	2.60	65.72
2	1451.86	1457.64	14	2.65	2.61	2.62	60.72	10.72	76.54	10.75	39.28	35.27
3	1478.10	1484.70	4	2.67	2.62	2.64	2.14	0.73	77.69	56.02	1.28	66.74

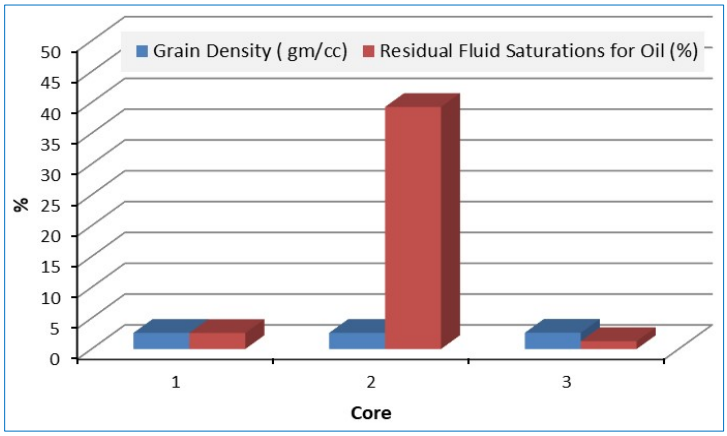

Fig. 7. Histogram showing the relation between grain density and residual fluid saturation for oil

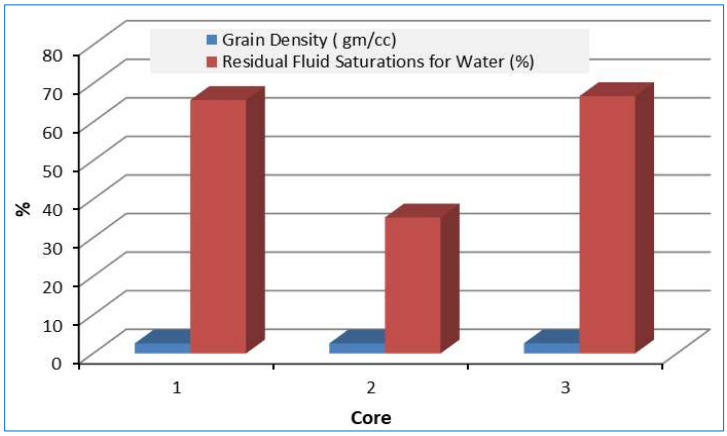

Fig. 8. Histogram showing the relation between grain density and residual fluid saturation for water

6. Conclusion

The study area is in the central part of the Rawat, a late Cretaceous to early Tertiary rift basin in interior Sudan. The basin lies to the north of the prolific NW-SW trending Melut Basin that formed due to extensional tectonics in the White Nile Cretaceous rift system in the Republic of South Sudan. The conventional core analyses study for the selected core plug samples from the cored intervals Core #1 (1441.30–1446.43 m), Core#2 (1451.86–1457.64 m) and Core#2 (1478.10–1484.70 m) showed a very good reservoir quality. The above core plug samples showed the following results:

- The helium porosity value for the studied plug samples ranged between 16.91% and 38.43%.
- The gas permeability value for the studied plug samples ranged between 7.09 to 1668.59 MD
- The residual fluid saturation values varied from 0.43% to 60.72 % for oil and 10.75 % to 77.69% for water.
- The grain density values varied from 2.61 g/cc to 2.67 g/cc.

References

Awad, M.Z., 1994. Stratigraphic, palynological and paleoecological studies in the East-Central sudan (Khartoum and kosti basin), Late Jurassic to Mid Tertiary.

Bosworth, W., 1992. Mesozoic and early Tertiary rift tectonics in east Africa.- In: C.J. Ebinger, H.K. Gubta and I.O. Nyambok (eds.), Seismology and Related Sciences in Africa. Tectonophysics 209, 115-137.

Bussert, R., 1993. Evolution of Cretaceous Continental basins in The Northen Sudan. Thorweihe and Scandelmeir (eds), Balkema Rotterdam p.407-415.

Catuneanu, O., 2002. Sequence stratigraphy of clastic systems: concepts, merits, and pitfalls. Journal of African Earth Sciences 35, 1-43. https://doi.org/10.1016/S0899-5362(02)00004-0.

Dolson, J.C., Bahorich, M.S., Tobin, R.C., Beaumont, E.A., Terlikoski, L.J., Hendricks, M.L., 2005. Exploring for Stratigraphic Traps, p. 21-68. Available on: https://www.searchanddiscovery.com/documents/halbouty03/images/ch21.pdf.

Dolson, J., He, Z., Horn, B.W., 2018. Advances and Perspectives on Stratigraphic Trap Exploration-Making the Subtle Trap Obvious, Search and Discovery.

Esawi, A.A., 2007. Palynological and paleoenviromental Interpretation of the late Certaceous to Tertiary strata of the Melut Basin (southeast Sudan). Unpublished PhD Thesis.

Halbouty, M.T., 1981. The Time Is Now for All Explorationists to Purposefully Search for the Subtle Trap: American Association of Petroleum Geologists Bulletin, p. 1-10.

Hassan, M.Z., 2016. Sedimentary Facies and TectonoStratigraphy of the Late Cretaceous-Neogene, of Rawat Basin White Nile State, Sudan. Master Thesis.

Jenkins, C.C., Duckett, A., Boyett, B.A., Glenton, P.N., Mills, A.A., Schapper, M.C., McPherson, J.G., Williams, M.A., 2017.

The Jansz-lo gas field, northwest shelf Australia: A giant stratigraphic trap, in R. K. Merrill and C. A. Sternbach, eds., Giant fields of the decade 2000–2010. AAPG Memoir 113, 305-326.

Jia, J., L., Z., Miao Z., Fank, S., Zhou, R., Meng, Q., Chen, Y., Yan, L., Yang, D., 2014. Depositional model and evolution for a deep-water sublacustrine fan system from the syn-rift Lower Cretaceous Nantun Formation of the Tanan Depression (Tamtsag Basin, Mongolia). Marine and Petroleum Geology 57, 264-282. https://doi.org/10.1016/j.marpetgeo.2014.05.022.

Lin, C., Eriksson, K., Sitian, L., Yongxian, W., Jianye, R., Yanmei, Z., 2001. Sequence architecture, depositional systems, and controls on development of lacustrine basin fills in part of the Erlian basin, northeast China. AAPG Bulletin 85, 2017-2043.

Salama, R.B., 1984. Buried troughs, grabens and rifts in Sudan. School of Applied Geology, University of New South Wales, Kensington 2033, New South Wales, Australia.

Salama, R.B., 1997. Rift Basins of the Sudan. In: Selley, R.C. (Ed.), Sedimentary Basins of the World, African Basins, vol. 3. Elsevier, Amsterdam, pp. 105e147.

Schull, T.J., 1988. Rift Basins of interior Sudan: Petroleum exploration and discovery. AAPG Bulletin 72, 1128-1142. https://doi.org/10.1306/703C9965-1707-11D7-8645000102C1865D.

Simm, R., Bacon, M., 2014. Seismic Amplitude: an interpreter's handbook. Cambridge University Press, 1-253.

Whiteman, A.J., 1971. The geology of the Sudan Republic. London Clarendon Press: Oxford, 290 pp.

Wycisk, P., Klitzsch, E., Jas, C., Reynolds, O., 1990. Intracratonal sequence development and structural control of Phanerozoic strata in Sudan. Berlin: Berliner geowissenschaftliche Abhandlungen.

Wycisk, P., Klitzsch, E., Jas, C., Renolds, O., 1990. Intracratonal Sequence development and structural control of phanerozoic strata in Sudan. Berliner geowissensch aft lische, Reihe A120, 45-86.

Zhu, H., Li, S., Shu, Y., Yang, X., Mei, L., 2016. Applying seismic geomorphology to delineate switched sequence stratigraphic architecture in lacustrine rift basins: An example from the Pearl River Mouth Basin, northern South China Sea. Marine and Petroleum Geology 78, 785-796. https://doi.org/10.1016/j.marpetgeo.2015.12.013.